Oil Shale, 2016, Vol. 33, No. 1, pp. 45–57
doi: 10.3176/oil.2016.1.04
ISSN 0208-189X


# NUMERICAL SIMULATION OF IN SITU CONVERSION OF CONTINENTAL OIL SHALE IN NORTHEAST CHINA

HAN HUI[a,b], ZHONG NING-NING[b]*, HUANG CAI-XIA[b], LIU YAN[b,c], LUO QING-YONG[b], DAI NA[b], HUANG XIAO-YAN[b,d]

[a] School of Geoscience and Technology, Southwest Petroleum University, Chengdu 610500, China
[b] State Key Laboratory of Petroleum Resources and Prospecting, China University of Petroleum, Beijing 102249, China
[c] College of Computer Science, Yangtze University, Jingzhou 434023, China
[d] Chongqing Institute of Geology & Mineral Resources, Chongqing 400042, China

***Abstract.*** *A numerical simulation of in situ conversion of continental oil shale in Northeast China was performed. Firstly, the transient temperature field of in situ conversion was calculated. Secondly, the apparent kinetic parameters from thermogravimetric experiments on continental oil shale were obtained. At last, the transformation rates of oil shale at different heating times were calculated applying apparent kinetic parameters to the heating rate obtained in the first step. The results demonstrated that continental oil shale needs to be heated for about 6–8 years to enable its conversion more than 90% under in situ retorting.*

***Keywords****: oil shale, in situ conversion, numerical simulation, temperature field, kinetics.*

## 1. Introduction

Oil shale is an organic-rich sedimentary rock that contains significant amounts of kerogen and can generate oil upon pyrolysis or retorting [1, 2]. Oil shale resource is enormous on Earth [3]. Man got oil from oil shale a long time ago already [4, 5]. A deposit of oil shale having economic potential is usually the one that is at or near enough to the surface to be developed by open-cast or conventional underground mining or by in situ methods [3]. Costs and environmental issues tend to favor in situ processes [6].

* Corresponding author: e-mail *nnzhongxp@cup.edu.cn*

There are several methods of in situ retorting for oil shale, such as Shell's in situ Conversion Process (ICP), ExxonMobil's Electrofrac$^{TM}$ Process, PetroProbe, Raytheon-CF Radio-Frequency with Critical Fluids Technology, and IEP's Geothermic Fuel Cell [7]. Compared with other technologies, the heating mode and construction process of ICP are simpler and its thermal efficiency is higher [8]. The technology was investigated extensively by Harold [9]. Predicting the in situ conversion process is significant to optimize the production plan. Because the in situ retorting of oil shale may take several years [9], it is time-consuming to simulate this process through pilot tests. Fortunately, numerical simulation provides an inexpensive and time-saving approach to research the process.

Computer models applicable to in situ oil shale retorting have been reported and used to analyze bench scale and field pilot tests under various conditions [10–16]. However, the above simulation was performed on marine Green River oil shale in the western United States. Since continental and marine oil shales differ in organic matter content, heat conductivity, specific heat, etc., the simulation results obtained may not be applicable to continental oil shale.

In this paper, a numerical simulation of the in situ retorting of continental oil shale in Northeast China was performed. In the simulation, we provided the retorting rates at various heating times. The results may be useful to apply in situ retorting to continental oil shale and modify the production plan.

## 2. Methods

### 2.1. Overview

In order to simulate in situ retorting of oil shale, the following procedures were performed in this study. Firstly, the temperature curves during in situ retorting were calculated by the Ansys simulator, and the heating rate was obtained. Secondly, the kinetic parameters were obtained from pyrolysis experiments using thermogravimetric apparatus. At last, the kinetic parameters were applied to the heating rate calculated in the first step to get conversion at different heating times. A detailed description of the three procedures will be given below.

### 2.2. Simulation of temperature field

In situ retorting employs well grids of different patterns, such as triangle pattern, square pattern, and hexagon pattern. Oil shale is heated uniformly in a triangle grid which is more efficient than grids of other patterns [17]. Therefore, a grid of this pattern was adopted in the current study. Three heaters formed a triangle, the distance between them was 30 m, in the center of the triangle there was a producer (Fig. 1). The heater temperature was assumed to be 750 °C, the initial temperature of oil shale was 20 °C.

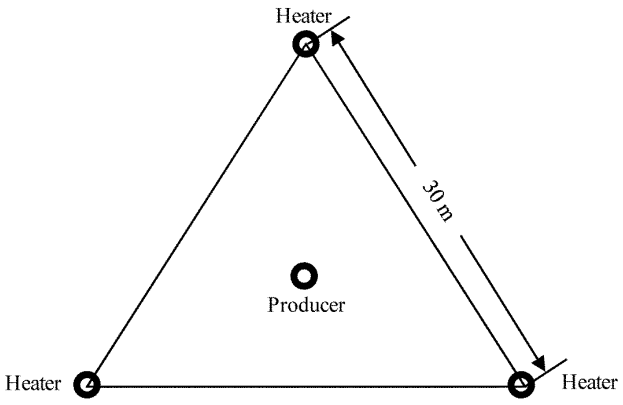


Fig. 1. A triangle grid.

In this study, temperature field simulation was performed using the Ansys simulator. In order to determine heat conduction, an energy balance equation was given by:

$$[C]\{T'\} + [K]\{T\} = \{Q\}, \quad (1)$$

where C is the specific heat matrix, T is the temperature vector, $T'$ is the derivative matrix of temperature with time, K is the conduction matrix, including thermal conductivity and shape factor, and Q is the heat flux vector.

The density, thermal conductivity and specific heat of continental oil shale in Northeast China were 2500 $g \cdot cm^{-1}$, 2.0 $W \cdot m^{-1}$ and 2.0 $J \cdot g^{-1} \cdot K^{-1}$, respectively [18].

### 2.3. Oil shale samples and their pyrolysis kinetics

In the process of in situ retorting of oil shale, the temperature, time and transformation efficiency depend on the kinetic parameters of oil shale pyrolysis and temperature field. Therefore, it is essential to obtain kinetic parameters from pyrolysis to understand the transformation mechanism and get parameters for numerical simulation.

In Northeast China, there are a few Cenozoic basins containing oil shale, the Yilan, Fushun, Huadian and Laoheishan basins are the major ones [19]. The Dalianhe Formation of Eocene in the Yilan Basin is composed of interbedded coal and oil shale. The oil shale in the basin has low oil content. The Eocene Guchengzi, Jijuntun and Xiloutian formations of the Fushun Basin consist of thick massive coal and oil shale. The Eocene Huadian Formation in the Huadian Basin comprises oil shale and silty shale. The many-layered oil shale of this formation has high oil content [20]. The Cretaceous oil shale in the Laoheishan Basin is thin, but of high oil content. In this study, we collected oil shale samples from the Dalianhe, Fushun, Huadian and Laoheishan basins (Table 1).

**Table 1. Geochemical parameters of different oil shales**

| Oil shale sample | TOC, % | $S_1$, mg/g | $S_2$, mg/g | $T_{max}$, °C | HI, mg/g |
|---|---|---|---|---|---|
| Dalianhe | 20.91 | 2.74 | 37.89 | 407 | 181 |
| Fushun | 10.84 | 1.47 | 34.02 | 430 | 314 |
| Huadian | 10.97 | 1.43 | 73.48 | 442 | 670 |
| Laoheishan | 48.69 | 1.55 | 56.88 | 402 | 117 |

The selected samples were ground (< 200 mesh) to eliminate the effect of heat and mass transfer on kinetic parameters. Then the samples were dried at a constant temperature of 80 °C for 3 hours to eliminate moisture. We performed TGA experiments using a Netzsch STA/449F3 thermogravimetric instrument (Germany). 20 mg samples were subjected to heating at the heating rates of 10, 20, 30 and 40 °C/min (Fig. 2). Argon was used at 50 ml/min up to 600 °C.

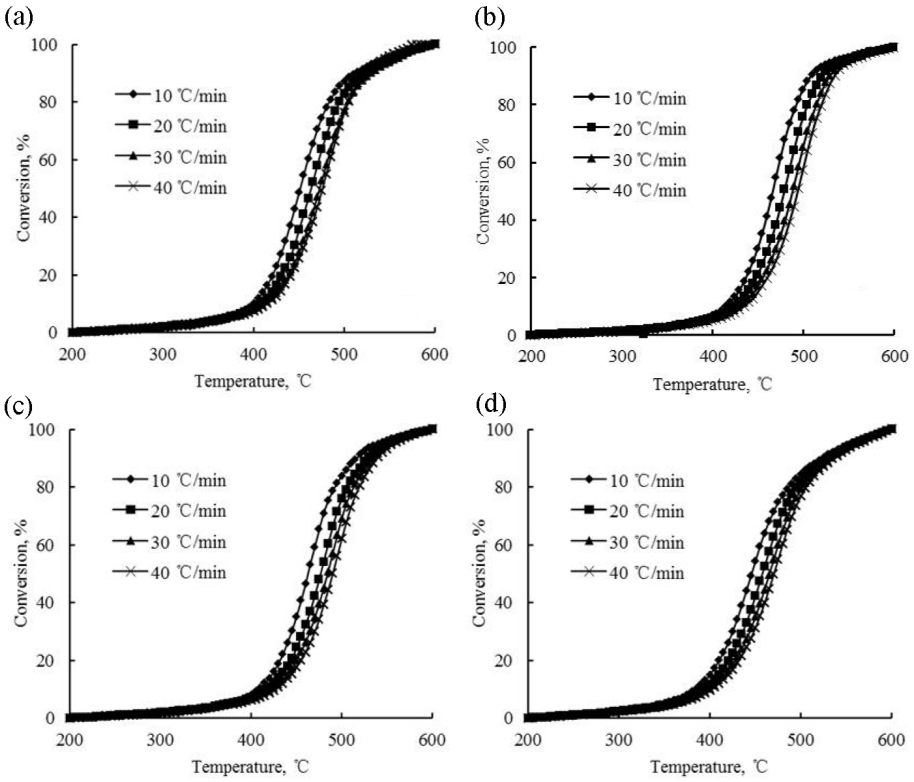


Fig. 2. Transformation ratios from experiment vs temperature for different oil shales: (a) Dalianhe, (b) Fushun, (c) Huadian, (d) Laoheishan.

According to the reaction rate theory, the kinetic equation for oil shale pyrolysis can be written as:

$$\frac{dx}{dt} = k(1-x)^n, \tag{2}$$

where $x$ is the degree of advance, $t$ is time, and $k$ represents the Arrhenius equation.

The Arrhenius equation is:

$$k = Ae^{-E/RT}, \tag{3}$$

where $E$ is the apparent activation energy, $A$ is the frequency factor, $T$ is temperature, and $R$ is the gas constant ($R$ = 8.314 J/mol K).

Inserting Equation (3) into Equation (2) will give:

$$\frac{dx}{dt} = Ae^{-E/RT}(1-x)^n. \tag{4}$$

If $n$ = 1, Equation (3) can be written as follows:

$$\frac{dx}{dT} = \frac{A}{D}e^{-E/RT}(1-x). \tag{5}$$

From Equation (4) and the constant heating rate ($dT/dt = D$), the differential kinetic model can be obtained:

$$\ln\left[\frac{dx}{dT}\cdot\frac{1}{1-x}\right] = \ln\frac{A}{D} - \frac{E}{RT}. \tag{6}$$

The linear regression of $\ln\left[\frac{dx}{dT}\cdot\frac{1}{1-x}\right]$ vs $1/T$ will give the apparent activation energy $E$ and the apparent frequency factor $A$.

### 2.4. Numerical simulation of oil shale in situ conversion

As there is a compensation relationship between temperature and time in organic matter pyrolysis, the kinetic parameters obtained from pyrolysis can be applied to geological conditions [21, 22]. Such an application of kinetic parameters is widely accepted in petroleum geology. In the process of ground retorting, oil shale needs be heated up to 500 °C to produce shale oil [23]. However, the heating rate upon in situ conversion is much lower than that by ground retorting; the former process may take several years and shale oil can be produced at a lower temperature [9]. Based on temperature field and kinetic parameters, we obtained the transformation curves vs. temperature and time by extrapolating kinetic parameters into the heating rate of in situ conversion. As the kinetic parameters obtained were apparent, the simulation results were approximate.

## 3. Results and discussion

### 3.1. Temperature field

Figure 3 shows the distribution of temperature field at various heating times. It can be seen that the temperature rose with time. The shorter the distance

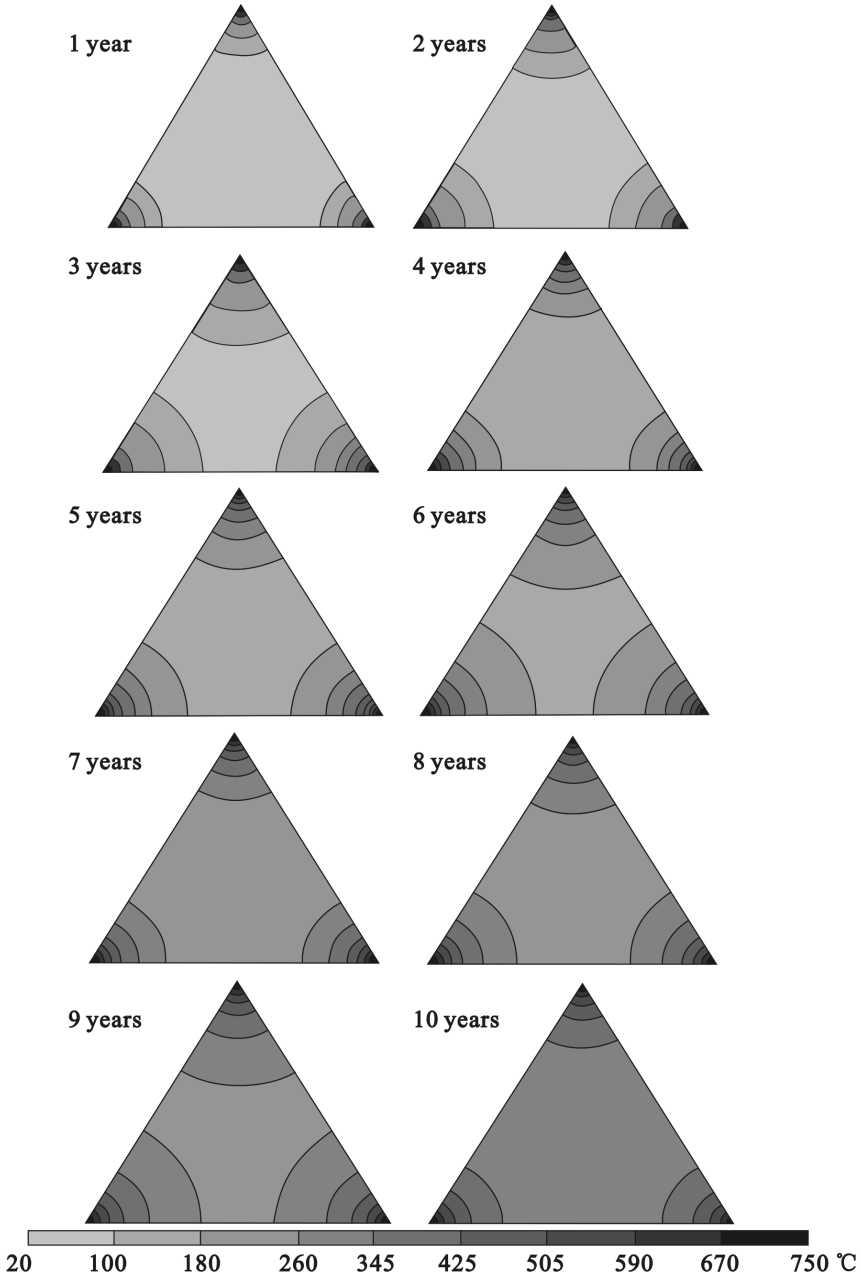


Fig. 3. Temperature field at different heating times.

between the heaters was, the more quickly the temperature increased (Figs. 4, 5). After heating oil shale for 10 years, the temperature of the whole triangle area was higher than 265 °C (Figs. 4, 5, 6). Figure 7 shows that the heating rate decreased with time, it was above 0.1 °C/day in the first two years. The heating rate was below this value in the following years, the average heating rate being between 0.05 and 0.1 °C/day. After a 3-year heating the heating rate of oil shale did not exceed the average (Fig. 7).

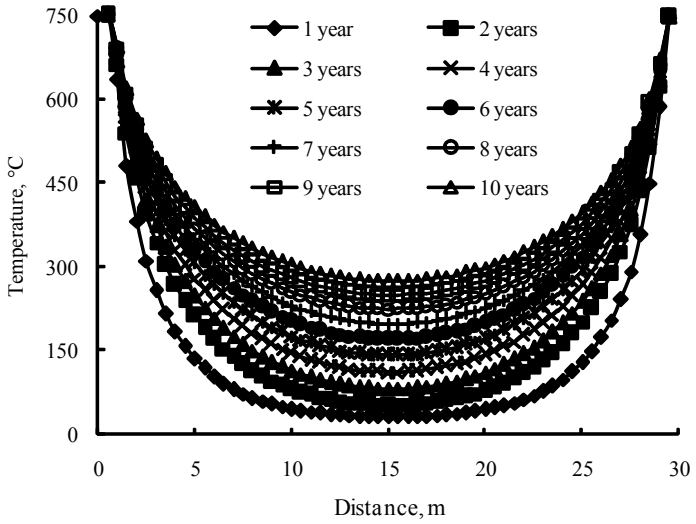


Fig. 4. Change of the temperature of heaters with time (the abscissa is the distance of producer from one heater).

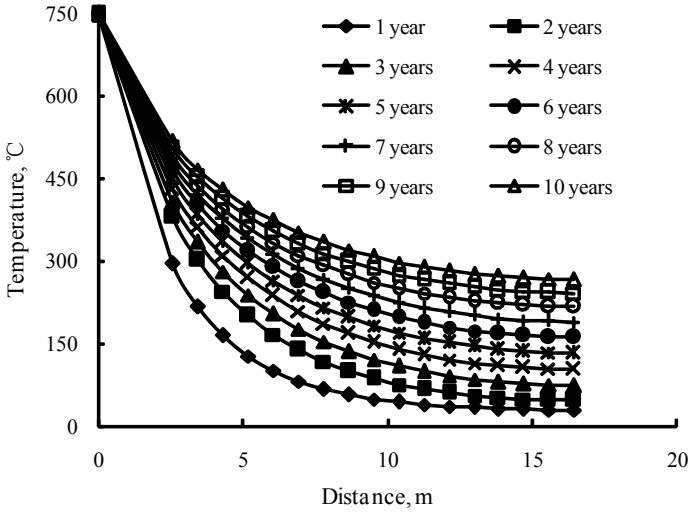


Fig. 5. Change of the temperature of heater and producer with time (the abscissa is the distance of producer from one heater).

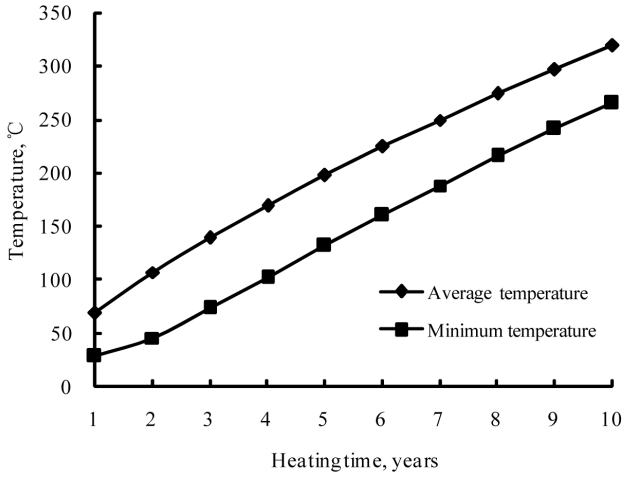


Fig. 6. Variation of average and minimum temperatures with time.

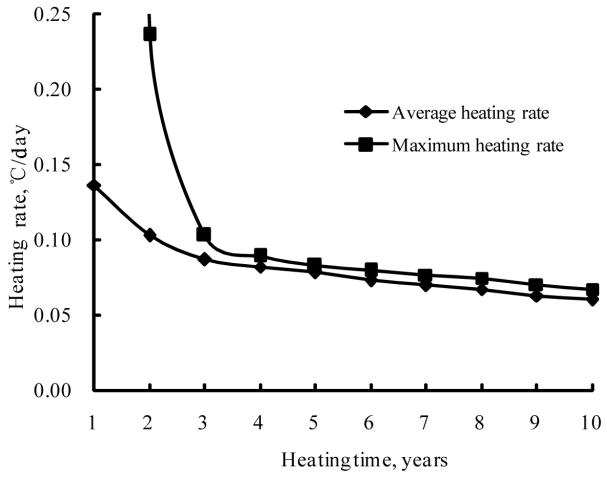


Fig. 7. Variation of heating rate with time.

### 3.2. Kinetic parameters

Table 2 presents the apparent kinetic parameters for pyrolysis of different oil shale samples. It can be seen that the apparent activation energies ranged from 118.18 kJ/mol to 156.21 kJ/mol, with an average of 137.56 kJ/mol. The apparent frequency factors varied between $1.27 \times 10^8$ $s^{-1}$ and $3.73 \times 10^{10}$ $s^{-1}$ and averaged $7.08 \times 10^9$ $s^{-1}$. The apparent activation energies of Fushun oil shale sample are similar to the corresponding values reported by Li and Yue [24]. In Figure 8 a kinetic compensation effect (KCE) is depicted. It is seen from the figure that there is a good linear relationship between the logarithm of frequency factor and activation energy. A similar linear relationship has been found for many other oil shale samples [23, 25–27]. Figure 9 shows

comparatively measured data and calculated values of conversion of different oil shale samples. It can be seen that the measured transformation ratio values agree with calculated ones, which indicates that the kinetic parameters can describe the pyrolysis of oil shale quite well.

**Table 2. Kinetic parameters for oil shale pyrolysis**

| Oil shale sample | Heating rate, °C/min | $E$, kJ·mol$^{-1}$ | $A$, s$^{-1}$ | $R$ |
|---|---|---|---|---|
| Dalianhe | 10 | 137.65 | 1.70E + 09 | 0.9804 |
| | 20 | 140.95 | 3.86E + 09 | 0.9772 |
| | 30 | 136.91 | 2.23E + 09 | 0.9865 |
| | 40 | 142.44 | 6.92E + 09 | 0.9904 |
| Fushun | 10 | 141.12 | 1.84E + 09 | 0.9669 |
| | 20 | 152.65 | 1.63E + 10 | 0.9823 |
| | 30 | 152.79 | 1.93E + 10 | 0.9890 |
| | 40 | 156.21 | 3.73E + 10 | 0.9930 |
| Huadian | 10 | 130.12 | 3.18E + 08 | 0.9595 |
| | 20 | 135.61 | 1.02E + 09 | 0.9668 |
| | 30 | 146.05 | 7.14E + 09 | 0.9858 |
| | 40 | 145.70 | 7.56E + 09 | 0.9896 |
| Laoheishan | 10 | 118.18 | 7.04 E + 07 | 0.9834 |
| | 20 | 119.55 | 1.27E + 08 | 0.9874 |
| | 30 | 122.54 | 2.60E + 08 | 0.9923 |
| | 40 | 122.52 | 3.07E + 08 | 0.9923 |

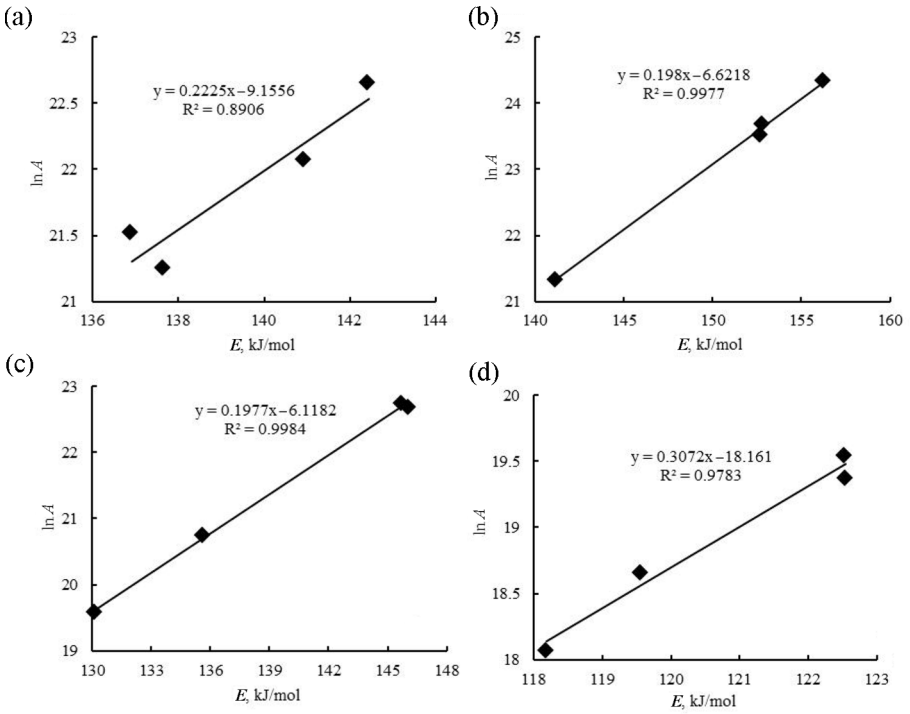


Fig. 8. ln$A$ vs $E$ curves for different oil shales: (a) Dalianhe, (b) Fushun, (c) Huadian, (d) Laoheishan.

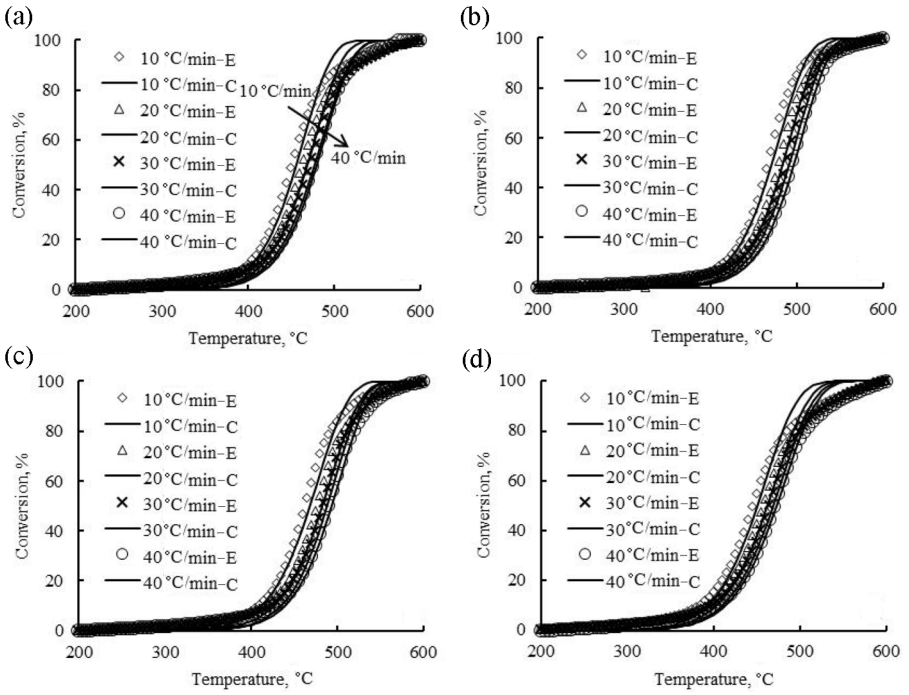


Fig. 9. Measured data vs calculated values for conversion of different oil shales: (a) Dalianhe, (b) Fushun, (c) Huadian, (d) Laoheishan.

### 3.3. Transform rates of in situ conversion

The simulation results showed that the heating rate was higher than 0.1 °C/day in the first two years, then it decreased slowly, the average heating rate varied between 0.05 and 0.1 °C/day (Fig. 7). To simplify calculations, we used an average heating rate of 0.075 °C/day. The results indicated that four oil shale samples had similar transformation vs. temperature curves, 10%–90% of transformation occurred within the time ranges of 6.2–7.7, 6.6–8.0, 6.0–7.7 and 5.3–6.8 years, respectively (Fig. 10). Symington and Spieker proposed that more than 90% of oil shale would be transformed after 7 years, our results were similar to theirs [15].

## 4. Conclusions

1. Temperature field simulation indicated the temperature of oil shale for in situ retorting to be above 265 °C after heating it for 10 years. With increasing heating time the heating rate decreased gradually, remaining stable thereafter.
2. The apparent activation energies calculated from oil shale pyrolysis experiments were about 118.18–156.21 kJ/mol, and the apparent frequency factors ranged from $1.27 \times 10^8$ $s^{-1}$ to $3.73 \times 10^{10}$ $s^{-1}$.

3. For in situ retorting, 10–90% transformation of oil shale would occur after heating it for 5–8 years. This result would be of help in designing in situ conversion and assessing its applicability to continental oil shale.

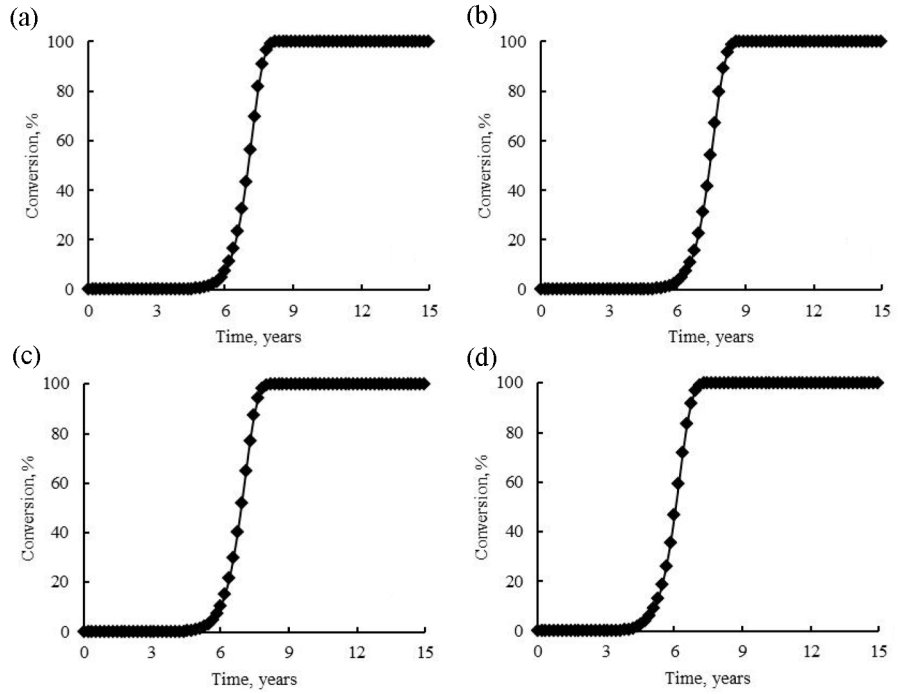


Fig. 10. Transformation ratios vs simulation time for different oil shales: (a) Dalianhe, (b) Fushun, (c) Huadian, (d) Laoheishan.

## Acknowledgements

This work was funded by Chinese National Key Science and Technology Special Project (Grant No. 2011ZX05018-002) and the Young Scholars Development Fund of SWPU (201499010088).

## REFERENCES

1. *UN Oil Shale and Tar Sands Panel. Final Report of the Technical Panel on Oil Shale and Tar Sands*. A/Conf. 100/PC/26, United Nations General Assembly, Geneva, 1981.
2. Peters, K. E., Walters, C. C., Moldowan, J. M. *The Biomarker Guide*. Second edition. Cambridge University Press, Cambridge, 2005.
3. Dyni, J. R. Geology and resources of some world oil-shale deposits. *Oil Shale*, 2003, **20**(3), 193–252.

4. Tissot, B. P., Welte, D. H. *Petroleum Formation and Occurrence*. Second edition. Springer Verlag, Germany, 1984.
5. Altun, N. E., Hicyilmaz, C., Hwang, J.-Y., Bagci, A. S. Evaluation of a Turkish low quality oil shale by flotation as a clean energy source: material characterization and determination of flotation behavior. *Fuel Process. Technol*., 2006, **87**(9), 783–791.
6. Zhang, F., Parker, J. C. An efficient modeling approach to simulate heat transfer rate between fracture and matrix regions for oil shale retorting. *Transport Porous Med*., 2010, **84**(1), 229–240.
7. Crawford, P. M., Biglarbigi, K., Dammer, A. R., Knaus, E. Advances in world oil shale production technologies. In: *SPE Annual Technical Conference and Exhibition (ATCE 2008)*, September 21–24, 2008 Denver, Colorado, USA, vol. 6, SPE 116570, 4101–4111.
8. Yang, H., Gao, X., Xiong, F., Zhang, J., Li, Y. Temperature distribution simulation and optimization design of electric heater for in-situ oil shale heating. *Oil Shale*, 2014, **31**(2), 105–120.
9. Harold, J. Heat sources with conductive material for in situ thermal processing of an oil shale formation. *United States Patent, 6929067*. 2005-08-16.
10. George, J. H., Harris, H. G. Mathematical modeling of in situ oil shale retorting. *SIAM J. Numer. Anal*., 1977, **14**(1), 137–151.
11. Gregg, M. L., Cambell, J. H., Taylor, J. R. Laboratory and modelling investigation of a Colorado oil-shale block heated to 900 °C. *Fuel*, 1981, **60**(3), 179–188.
12. Campbell, J. H., Gallegos, G., Gregg, M. Gas evolution during oil shale pyrolysis. 2. Kinetic and stoichiometric analysis. *Fuel*, 1980, **59**(10), 727–732.
13. Braun, R. L., Diaz, J. C., Lewis, A. E. Results of mathematical modeling of modified in-situ oil shale retorting. *Soc. Petrol. Eng. J*., 1984, **24**(01), 75–86.
14. Parker, J. C., Zhang, F. Efficient formulations of heat and mass transfer in oil shale retort models. *26th Oil Shale Symposium, Colorado School of Mines, 16–19 October 2006*, Colorado, USA.
15. Symington, W. A., Spiecker, P. M. Heat conduction modeling tools for screening *in situ* oil shale conversion processes. *28th Oil Shale Symposium, Colorado School of Mines, October 13–15, 2008*, Colorado, USA.
16. Fan, Y., Durlofsky, L. J., Tchelepi, H. Numerical simulation of the in-situ upgrading of oil shale. *SPE Reservoir Simulation Symposium, The Woodlands, Texas, USA, 2–4 February 2009*, SPE Paper 118658, Texas, 2009.
17. Wellington, S. L., Berchenko, I. E., Rouffignac, E. P., Fowler, T. D., Ryan, R. C., Gordon Jr., T. S., Stegemeier, G. L., Vinegar, H. J., Zhang, E. In situ thermal processing of an oil shale formation to produce a desired product. *US Patent, 2003/0136558 A1*. 2003-07-24.
18. Kang, Zhi-qin, Zhao, Yang-sheng, Yang, Dong. Physical principle and numerical analysis of oil shale development using in-situ conversion process technology. *Acta Petrolei Sinica*, 2008, **29**(4), 592–595 (in Chinese).
19. Liu, Z., Meng, Q., Jia, J., Sun, P., Liu, R., Hu, X. Metallogenic regularity of oil shale in continental basin: case study in the Meso-Cenozoic basins of Northeast China. *Journal of Jilin University, Earth Science Edition*, 2012, **42**(5), 1286–1297 (in Chinese).
20. Liu, R. *Research on Oil Shale Characteristics and Metallogenic Mechanism of Cenozoic Fault Basins in Eastern Northeast Region*. PhD Thesis, Changchun: Jilin University, 2007 (in Chinese).

21. Ungerer, P., Pelet, R. Extrapolation of the kinetics of oil and gas formation from laboratory experiments to sedimentary basins. *Nature*, 1987, **327**, 52–54.
22. Tissot, B. P., Pelet, R., Ungerer, P. Thermal history of sedimentary basins, maturation indices, and kinetics of oil and gas generation. *AAPG Bull*., 1987, **71**, 1445–1466.
23. Johannes, I., Zaidentsal, A. Kinetics of low-temperature retorting of kukersite oil shale. *Oil Shale*, 2008, **25**(4), 412–425.
24. Li, S., Yue, C. Study of different kinetic models for oil shale pyrolysis. *Fuel Process. Technol*., 2003, **85**(1), 51–61.
25. Li, S., Yue, C. Study of pyrolysis kinetics of oil shale. *Fuel*, 2003, **82**(3), 337–342.
26. Johannes, I., Kruusement, K., Veski, R. Evaluation of oil potential and pyrolysis kinetics of renewable fuel and shale samples by Rock-Eval analyzer. *J. Anal. Appl. Pyrol*., 2007, **79**(1–2), 183–190.
27. Xue, H., Li, S., Wang, H., Zheng, D., Fang, C. Pyrolysis kinetics of oil shale from northern Songliao basin in China. *Oil Shale*, 2010, **27**(1), 5–16.

*Presented by Ü. Rudi*
Received January 5, 2015